

Imbalancing the DNA Base Excision Repair Pathway in the Mitochondria; Targeting and Overexpressing *N*-Methylpurine DNA Glycosylase in Mitochondria Leads to Enhanced Cell Killing¹

Melissa L. Fishel, Young R. Seo, Martin L. Smith, and Mark R. Kelley²

Departments of Pediatrics [M. L. F., M. R. K.] and Biochemistry and Molecular Biology [M. L. F., M. R. K.], Herman B. Wells Center for Pediatric Research [M. L. F., M. R. K.], and Department of Microbiology [Y. R. S., M. L. S.], Indiana University School of Medicine, Indianapolis, Indiana 46202

ABSTRACT

The DNA base excision repair (BER) pathway is responsible for the repair of alkylation and oxidative DNA damage. The short-patch BER pathway, beginning with the simple glycosylase *N*-methylpurine DNA glycosylase (MPG), is responsible for the removal of damaged bases such as 3-methyladenine and 1,*N*⁶-ethenoadenine from the DNA after alkylation or oxidative DNA damage. The resulting apurinic site is further processed by the other members in the pathway, resulting in the insertion of the correct nucleotide. If apurinic sites accumulate, they are mutagenic and cytotoxic to the cell. To evaluate its efficacy in sensitizing breast cancer cells to chemotherapy, MPG has been overexpressed in the breast cancer cell line, MDA-MB231. With MPG overexpression, an increase in DNA damage and increased cytotoxicity to methyl methanesulfonate as well as increased apoptosis levels was observed in these cells. Because mitochondrial DNA has been shown to be more sensitive to DNA damage than nuclear DNA, a construct containing mitochondrial-targeted MPG using the human manganese superoxide dismutase mitochondrial-targeting sequence was made. Overexpression of the mitochondrially targeted MPG dramatically increased the breast cancer cells' sensitivity to methyl methanesulfonate. In conclusion, we believe that the increase in sensitivity to DNA damage by overexpression of nuclear MPG is because of an imbalance in the BER pathway, and an even greater increase in cell sensitivity is observed when mitochondrial DNA is targeted.

INTRODUCTION

DNA glycosylases, which initiate repair in the DNA BER³ pathway, hydrolyze the *N*-glycosylic bond between the deoxyribose sugar moiety and the DNA base leaving an AP site (1). MPG is responsible for the removal of damaged purines such as 3-MeA, 3-methylguanine, 7-methylguanine, hypoxanthine, and ϵ A and is part of the short-patch BER pathway (Fig. 1). The BER pathway repairs AP sites and nucleotides that have been damaged by oxidation and/or alkylation and restores the chemical integrity of DNA. MPG is a simple glycosylase in that it cleaves the *N*-glycosylic bond between the deoxyribose sugar moiety and the DNA base that is damaged but does not nick the DNA backbone. After hydrolysis by a simple glycosylase, the resulting AP site is excised by Ape1/ref-1 (2, 3). Ape1/ref-1 nicks the

phosphodiester backbone 5' to the AP site, leaving a 3'-hydroxyl group and a 5'-deoxyribose phosphate group flanking the nucleotide gap (4–6). To complete short-patch repair, DNA polymerase β excises the 5'-deoxyribose phosphate moieties remaining after Ape1/ref-1 incision and inserts up to six new nucleotides (7–9). DNA ligase I or DNA ligase III/X-ray cross-species complementing 1 completes the repair process by sealing the resulting nick (10).

Repair systems for nuclear DNA are much better characterized than repair systems for mtDNA. The mtDNA genome is composed of 16,569 bp and encodes 13 polypeptides of the respiratory chain complex, 22 tRNAs, and 2 rRNAs (11). Additionally, mtDNA is very different from nuclear DNA; it does not contain long sequences of noncoding bases, contains no introns, and is not protected by histones (12). If mtDNA accumulates damage, the proteins involved in the electron transport chain are either not synthesized or mutant forms are synthesized. This accumulation of damage is believed to contribute to diabetes mellitus, cancer, ischemic heart disease, Alzheimer's disease, and aging (13–16). Repair of mtDNA is crucial based on the findings of several laboratories that mtDNA suffers more damage than nuclear DNA after treatment with oxidative or alkylating agents (17–21). In addition to being subjected to more damage, the mutation rate is also 5–10 times greater in mtDNA (22, 23). The repair of oxidative stress generated by the high levels of ROS does occur (24, 25), and mitochondria have also been shown to repair alkylation damage (12).

A simplified BER in mitochondria has been established but has not been extensively characterized. Several BER enzymes such as uracil DNA glycosylase (26) and AP endonuclease (27) have been detected in mitochondria (Fig. 1). The replication polymerase in mitochondria is γ (pol γ), and it has been demonstrated that purified pol γ can also serve as a repair polymerase in mitochondria (28, 29). The ligase involved in mitochondrial BER is believed to be an alternate splice variant of nuclear DNA ligase III (28). To date, there is no account of MPG in mitochondria. However, mitochondria from hamster cells have been shown to remove adducts caused by treatment with MMS (30), and mitochondria from a rat insulinoma cell line repaired adducts caused by streptozotocin (31). These agents generate lesions recognized and removed by MPG.

On the basis of overexpression experiments with other DNA repair proteins (32), a hypothesis was formed stating that the overexpression of MPG would result in more damaged bases removed, and the cells would show an increase in resistance to alkylating agents. However, in CHO cells, overexpression of human MPG resulted in hypersensitivity to MMS, Dimethyl Sulfate (DMS) (33), and *N*-methyl-*N*'-nitro-*N*-nitrosoguanidine (34). In addition to being more sensitive to alkylating agents, CHO cells that overexpressed MPG had a higher frequency of chromosomal aberrations, a stronger inhibition of DNA replication, and more double-strand breaks compared with control CHO cells (34). All of these results indicated an imbalance of DNA repair in the CHO cells with MPG overexpression in the nucleus.

To further this research and to better understand MPG's function in the repair of nuclear and mtDNA, we demonstrate that by targeting MPG to the mitochondria, the viability of the breast cancer cell line

Received 6/24/02; accepted 11/21/02.

The costs of publication of this article were defrayed in part by the payment of page charges. This article must therefore be hereby marked *advertisement* in accordance with 18 U.S.C. Section 1734 solely to indicate this fact.

¹This work was supported by NIH Grants CA76643 (to M. R. K.), NS38506 (to M. R. K.), P01-CA75426 (to M. R. K.), and a Department of Defense Congressionally Directed Medical Research Programs predoctoral fellowship BC991226 to (to M. F.). The Riley Memorial Association also supported this study.

²To whom requests for reprints should be addressed, at Jonathan and Jennifer Simmons Professor of Pediatrics and Professor, Department of Biochemistry and Molecular Biology, Wells Center for Pediatric Research, Indiana University School of Medicine, Herman B. Wells Center, Room 2600, 702 Barnhill Drive, Indianapolis, IN 46202. Phone: (317) 274-2755; Fax: (317) 274-5378; E-mail: mkkelley@iupui.edu.

³The abbreviations used are: BER, base excision repair; MPG, *N*-methylpurine DNA glycosylase; DPBS, Dulbecco's PBS; 3-MeA, 3-methyladenine; ϵ A, 1,*N*⁶-ethenoadenine; AP, apurinic/aprimidinic; Ape1/ref-1, AP endonuclease I/redox effector factor-1; mtDNA, mitochondrial DNA; nDNA, nuclear DNA; mito-MPG, mitochondria MPG; MMS, methyl methanesulfonate; AO, acridine orange; CHO, Chinese hamster ovary; PI, propidium iodide; MS, mannilol-sucrose; Annexin-V-FITC, fluorescein-conjugated Annexin-V; MX, methoxyamine; KF, killing factor; ROS, reactive oxygen species.

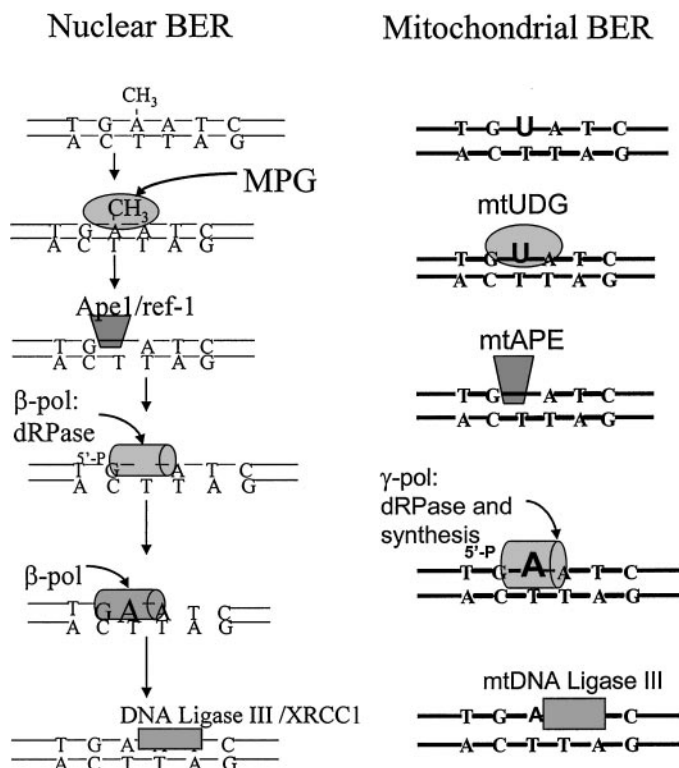


Fig. 1. The short-patch BER pathway in the nucleus and mitochondria.

MDA-MB231 is dramatically affected. The viability of MDA-MB231 cells that overexpressed nuclear MPG were also affected in response to alkylating agent MMS but not as dramatically as the cells that overexpressed mito-MPG. We also demonstrated that the cells were dying through an apoptotic pathway. Interestingly, the cells that expressed mito-MPG had a significant number of cells undergoing apoptosis even without drug treatment. These results indicate that the mitochondria is responsible for a significant amount of cell survivability, both in the presence of endogenous base damage, as well as after drug treatment. Furthermore, these data demonstrate that damaging mtDNA can lead to the initiation of apoptosis, *i.e.*, triggering apoptotic pathways from within the mitochondria instead of from the outside of the mitochondria. Finally, the targeting of selected DNA BER repair enzymes to the mitochondria leads to an imbalance of the BER repair pathway and increased cell death at lower doses than with nuclear imbalancing of BER. This approach could have usefulness in tumor targeted gene therapy approaches to sensitizing tumor cells to lower doses of chemotherapeutic agents with enhanced cell killing.

MATERIALS AND METHODS

Chemicals and Cell Lines. Chemicals and enzymes were purchased from Fisher Scientific (Pittsburgh, PA), Sigma (St. Louis, MO), and New England Biolabs (Beverly, MA). [α - 32 P]dCTP and [γ - 32 P]dATP were obtained from Amersham Pharmacia Biotech (Buckinghamshire, United Kingdom). The MDA-MB231 cell line was kindly provided by Dr. Martin Smith (Department of Microbiology, Indiana University School of Medicine). MDA-MB231 cells were maintained in RPMI media (Life Technologies, Inc., Gaithersburg, MD), supplemented with 10% fetal bovine serum (Hyclone Laboratories, Logan, UT), and 1% penicillin/streptomycin (Life Technologies, Inc.) in 5% CO₂ at 37°C. Transfections of the MDA-MB231 cells were performed when the cells were ~70% confluent with the Lipofectin reagent (Life Technologies, Inc.) according to the manufacturer's protocol. The transfected MDA-MB231 cells were put under selection in 1 mg/ml G418 (Geneticin; Life Technologies, Inc.) for 10 days and assayed for MPG expression.

Construction of Mitochondrial-targeted MPG into pCR2.1 Vector. The mitochondrial-targeting sequence originated from the human manganese superoxide dismutase enzyme (35, 36). To add the mitochondrial-targeting sequence to the 5' end of MPG (mito-MPG), a primer (AAGAATTCATGTGAGCCGGGCGAGTGTGCGGCACCAGCAGGCAGCTGGCTCCGGCTTTGGGTATCTGGGCTCCAGGCAGATGGTCACCCCGCTTTG) was constructed (36). This primer contains an *Eco*RI site (bold) and the mitochondrial-targeting sequence (italics). The following oligonucleotide was used as the 3' primer (ATCGGGCTCGAGTCAGGCCTGTGTGCTCCTGCTC) and contained an *Xho*I site. This PCR product was cloned into the pCR2.1 vector (TA cloning kit; Invitrogen, Carlsbad, CA). The mitochondrial-targeted MPG's sequence was confirmed using the DNA sequencing facilities at Biochemistry Biotechnology Facility at Indiana University School of Medicine.

Construction of Mitochondrial-targeted MPG. The human MPG gene had previously been cloned from HT-29 cells by reverse transcription-PCR, ligated into pAMP1 (Clone-AMP kit; Life Technologies, Inc.), and the correct sequence confirmed (Indiana University School of Medicine, Biochemistry Biotechnology Facility). The pAMP1 vector containing MPG was digested with *Eco*RI and *Xho*I (New England Biolabs). The MPG cDNA was ligated into the pcDNA3.1 vector using T4 DNA ligase (Life Technologies, Inc.; Fig. 2). To add the mitochondrial target to the 5'-end of MPG, primers were constructed as discussed above. These primers were used in a PCR reaction to amplify the MPG cDNA with the addition of the 72-bp mitochondrial-targeting sequence. After purification of the PCR product, it was ligated into a TA cloning vector, pCR2.1. The sequence of the mitochondrial target and the MPG gene were confirmed. MPG with the mitochondrial-targeting sequence was ligated into the mammalian expression vector pcDNA3.1 (Fig. 2). Confirmation of the insertion of mito-MPG into this vector was accomplished using PCR and restriction digestion. The expected ~1-kb fragment corresponding to mito-MPG was confirmed. As described previously, the MPG gene was excised from of the pAMP1 vector, moved into pcDNA3.1, and the correct sequence was confirmed. Again, to confirm that it was inserted into the pcDNA vector, PCR and restriction digestion were used. The expected ~900-bp fragment corresponding to MPG was evident by both methods (data not shown).

Northern Blot Analysis. Total cellular RNA was isolated from a confluent plate of cells using RNA Stat-60 (Tel-Test "B", Friendswood, TX) and the indicated manufacturer's protocol. A total of 20 μ g of RNA was electrophoresed in a 1.2% formaldehyde-agarose gel and transferred onto Hybond-N nylon membrane using 10 \times SSC (1.5 M NaCl, 0.15 M sodium citrate). The cDNA was labeled with [α - 32 P]dCTP using the DECAprime II DNA labeling kit (Ambion, Austin, TX) following the protocol indicated by the manufacturer.

Western Blot Analysis. Equal amounts of protein (20 μ g) were separated on a SDS/(12%)-polyacrylamide gel and transferred to a nitrocellulose filter. The Roche Chemiluminescence kit (Indianapolis, IN) was used for the blocking and detection reagents. Primary MPG polyclonal antibody was kindly provided by Dr. Tim O'Connor (Department of Biology, Beckman Research Institute), the cytochrome C monoclonal antibody was purchased from Pharmingen (San Diego, CA), and the monoclonal Apε1/ref-1 antibody (Novus Biologicals, Littleton, CO; Refs. 37, 38).

MPG Activity Assay. To assay the cells for MPG activity, an oligonucleotide-based assay, was developed similar to the well-established AP endonuclease

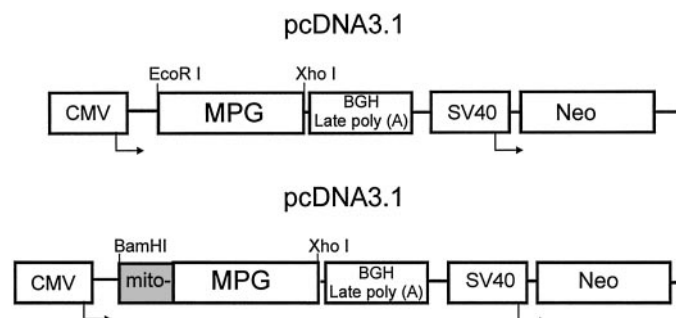


Fig. 2. Mito-MPG and nMPG constructs. The vector backbone was pcDNA 3.1, which drives mito-MPG or nMPG expression off the CMV promoter. Mito-MPG and MPG were cloned into the MCS.

oligonucleotide assay (39, 40). The oligo was synthesized by Midland Reagent Co. (Midland, TX) and included a ϵ A. The oligo containing the ethenoadenine had the following sequence: (5'-AATTCACCGGTACC(ϵ A)CCTAGAA-TTCG-3'), and the compliment oligo: (5'-CGAATTCTAGGTGGTACCGGT-GAATT-3'). Approximately 1 million cells were pelleted, washed in DPBS, resuspended in 1 \times PBS, 2 mM DTT, and sonicated on ice at 45 W for 30 s. The lysate was spun down at 12,000 rpm for 5 min. The amount of protein in the cell lysate was quantitated using the Bradford Protein Assay. Whole cell lysate (20 μ g of nMPG clones and 50 μ g of mito-MPG clones), MPG assay buffer [1 \times [25 mM HEPES-KOH (pH 7.8), 0.5 mM EDTA, 0.5 mM DTT, 150 mM KCl, 10% glycerol; Ref. 41], and 2.5 pmol of [γ - 32 P]dATP-labeled substrate were incubated at 37°C for 60 min. One volume of stop buffer (96% formamide, 10 mM EDTA, 0.1% xylene cyanol, 0.1% bromophenol blue) was added to the reaction. The samples were electrophoresed at 300 V for \sim 45 min on a 20% 7M Urea denaturing polyacrylamide gel and exposed to autoradiography film (Amersham Pharmacia Biotech).

Purification of Mitochondria. This protocol was provided by Allison Dobson from Dr. Glenn Wilson's laboratory (Department of Cell Biology and Neuroscience, University of South Alabama; Ref. 36). All supernatants and centrifugations in this procedure were incubated on ice or at 4°C. Briefly, to extract the mitochondria from the MDA-MB231 cells, \sim 5–6 million cells were collected, washed with DPBS, and lysed with 5 ml of ice-cold Digitonin [40 mg of digitonin/100-ml solution, 2.5 mM EDTA, 250 mM mannitol, 17 mM 4-morpholinepropanesulfonic acid (pH 7.4)]. Next, 2.5 \times MS buffer [525 mM mannitol, 175 mM sucrose, 12.5 mM Tris, 12.5 mM EDTA (pH 7.4)] was added to the homogenate. The homogenate was centrifuged at 800 \times g for 10 min (Beckman J2–21 Centrifuge, JA-17 rotor). The supernatant was transferred to a clean tube, and the pellet was resuspended in 1 \times MS. The solution was centrifuged again (10 min, 800 \times g) and resuspended in 1 \times MS as before. This step was repeated up to three times, and the combined supernatants were spun once more at 800 \times g to remove any remaining nuclei. That supernatant was transferred to a clean tube and spun for 20 min at 10,000 rpm (Beckman J2–21 Centrifuge, JA-17 rotor) or 10,000 \times g to pellet mitochondria. The mitochondrial pellet was lysed in the 1 \times protein loading dye used for Westerns. The protein was quantitated with the Bradford Protein assay, and Western blot analysis was performed as described previously.

Purification of Nuclear Extract. The Nuclei Pure Prep Isolation Kit from Sigma was used to purify nuclear extracts, and the manufacturer's indicated protocol was followed. Briefly, \sim 2–4 million cells were collected, washed with DPBS, and resuspended in ice-cold lysis solution (Nuclei PURE lysis buffer, 1 mM DTT, 0.1% Triton X-100). Centrifuging the cell lysate through a sucrose cushion solution then purified the nuclei. The nuclei were stored at -80°C until needed for Western blot analysis. The cells were lysed with 1 \times Protein Lysis buffer as previously described.

Cell Survival Assays Using the Colony Formation Assay. To evaluate cell survival after drug treatment, \sim 600,000 cells were plated on a 10-cm dish and allowed to attach overnight. The cells were treated with drug for 1 h, washed in DPBS, counted, and plated in triplicate at a density to give between 30 and 300 colonies/10-cm dish. After \sim 12 days, the plates were stained with methylene blue (0.5% methylene blue, 50% methanol), and the colonies were scored. Two formulas for cell survival were used to compare the 231+mito-MPG and the 231+nMPG cells. One formula compared MDA-MB231 cells with and without the transgene(s) and evaluated cell survival based on plating efficiency and their ability to form a colony after treatment using the following formula: average number of colonies/number of cells plated \times PE, where PE = number of colonies of untreated MDA-MB 231 cells/number of cells plated.

Annexin-V-FITC/PI Staining. To analyze the cells for apoptosis, \sim 600,000 cells were plated and allowed to attach overnight. Cells were continuously treated with the MMS for \sim 48 h and then assayed for apoptosis using Annexin-V-FITC staining (42). The cells were trypsinized, pelleted, washed in DPBS, and resuspended in 1 \times Binding Buffer [10 mM HEPES/NaOH (pH 7.4), 140 mM NaCl, 2.5 mM CaCl $_2$] containing Annexin-V-FITC antibody (PharMingen) and PI according to the manufacturer's indicated protocol. The samples were analyzed by flow cytometry.

Caspase-3 Activity Assays. The activation of the caspase cascade was measured through the caspase-3 enzyme activity in cell lysates. The fluorogenic substrate used in this assay was Ac-Asp-Glu-Val-Asp-AMC (Alexis Biochemicals, San Diego, CA) as described previously (43). AMC is 7-amido-

4-methylcoumarin, and caspase-3 cleaves between the Asp and the AMC. Briefly, the cells were treated continuously with MMS for \sim 48 h, trypsinized, pelleted, washed in DPBS, and lysed in lysis buffer (50 mM PIPES-OH, 50 mM KCl, 5 mM EGTA, 2 mM MgCl $_2$, 1 mM DTT). The cells resuspended in lysis buffer were incubated on ice and then spun down to pellet the cell debris. Reaction buffer (2 \times , 200 mM HEPES, 20% sucrose, 0.2% CHAPS, 0.2 mg/ml BSA, 20 mM DTT) and the fluorogenic substrate were added to each sample, and the reaction was incubated at 37°C for 1 h. Release of the fluorogenic AMC moiety was measured using a Hitachi F2000 Spectrophotometer (excitation, 380 nm; detection, 460 nm). The caspase-3-specific activity is in units of pmols of AMC/h/ μ g protein.

Cell Morphology and Confocal Microscopy. Nucleus fragmentation and chromatin condensation were used as morphological criteria of apoptosis to identify apoptotic cells with AO staining (44). Cells were treated with 0.2 mM MMS for \sim 48 h, washed with PBS, trypsinized, placed on microscope slides, and directly stained with AO (40 mg/ml in PBS). The images of apoptotic bodies in AO staining were taken with the LSM-510 confocal laser scanning microscope system (Carl Zeiss, Oberkochen, Germany).

Calculation of the KF. To better understand the cell survival curves for 231+mito-MPG and 231+nMPG cells, an arbitrary value, the KF, was assigned that is defined by the percentage of 231+mito-MPG and 231+nMPG cells that were killed divided by the units of MPG activity. For example, 231+mito-MPG cells at zero dose with 9.6 units of activity had a 56.58% kill, 231+nMPG cells at zero dose with 23.0 units of activity had a 23.19% kill, and these numbers correspond to a KF of 5.89 and 1.01, respectively.

Statistics. *P*s for the cell survival data were generated using the one-way ANOVA test with Sigma Stat software (Jandel Scientific, Erkrath, Germany). *P*s for the comparison of cell survival curves were generated by Dr. SinHo Jung (Department of Biostatistics, Indiana University School of Medicine). Dr. Jung used the χ^2 test with two degrees of freedom to compare the three slopes from the cell survival data of 231+pcDNA, 231+nMPG, and 231+mito-MPG. To compare the slopes of two of the cell lines, Dr. Jung used the standard *t* test.

RESULTS

Detection of Mito-MPG and MPG in the MDA-MB231 Cells.

To evaluate expression of mitochondrial-targeted MPG (231+mito-MPG) and nuclear MPG (231+nMPG), the cells were collected and analyzed by Northern and Western blot analysis and by the MPG activity assay. Northern blot analysis of the 231+mito-MPG cells demonstrated a band that was \sim 72 bp larger than nuclear MPG (data not shown). For Western blot analysis MPG protein was detected in the transfected cell lines (231+mito-MPG and 231+nMPG) at M_r \sim 36,000 as expected (Fig. 3A). There was nonspecific binding of the MPG polyclonal antibody to a protein that was M_r \sim 50,000 in size. This band was evident in all of the lanes of the Western blot illustrating equal loading of protein. The mitochondria were also collected from the cells that had been transfected with the mitochondrial-targeted MPG construct and analyzed for MPG protein demonstrating the presence of MPG in the mitochondria (Fig. 3B). MPG activity assays using an ϵ A substrate were also performed on whole cell lysates from the cell lines shown in Fig. 3A (Fig. 3C). To confirm that the mito-MPG was targeted to the mitochondria and not the nucleus, the mitochondrial preparation was analyzed using a cytochrome *c* antibody to demonstrate that the mitochondria isolation preparation was specific for mitochondria (Fig. 4A). Nuclear extracts were also prepared from these cells to demonstrate that the MPG was indeed targeted to the mitochondria in these cells (Fig. 4B). This same blot was probed with a monoclonal Ape1/ref-1 antibody to show that the nuclei were intact, and the lanes did contain protein. As shown in Fig. 4B, the MPG protein was barely detectable in the nuclei of the vector control (231+pcDNA) cells and in the nuclei of 231+mito-MPG clones no. 3 and no. 8. Fig. 4B, Lane 1, of the top panel demonstrated the expression of MPG in the mitochondria of 231+mito-MPG clone no. 8 for comparison of expression levels. The 231+mito-MPG and

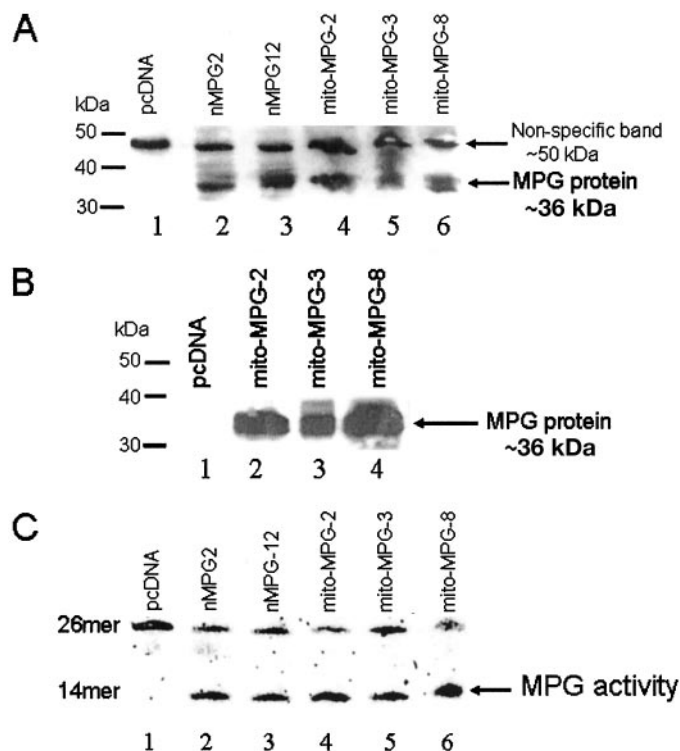


Fig. 3. Mito-MPG or nMPG expression in MDA-MB231 cells. **A**, Western blot analysis of protein (20 μ g) from the whole cell lysates of 231 cells with nMPG overexpression. **B**, Western blot analysis of protein (20 μ g) from the mitochondria of 231 cells with mito-MPG overexpression. **C**, MPG activity assay from whole cell extracts of 231 cells transfected with vector, MPG, and mito-MPG. Lane 1, MDA-231 cells transfected with pcDNA3 empty vector as a control.

the 231+nMPG cells were also analyzed by the MPG activity assay using whole cell lysates (Fig. 4, C and D; Table 1). Both sets of clones had significantly more MPG activity than the 231+pcDNA cells. (from reviewer no. 1, point 2, can discard if you want) The activity of nMPG clones was more than 2fold the activity of the mito-MPG clones. However the levels of exogenous protein as determined by Western blot look similar. This could be attributable to the activity assay was performed on whole cell lysates and the Western blot of the mito-MPG clones was loaded with only mitochondrial protein.

Colony Formation Assay of the MDA-MB231 Cells with Mito-MPG and MPG Overexpression. Colony formation assay was used to determine cell survival after treatment with MMS at doses of 0.05, 0.1, and 0.2 mM. The 231+mito-MPG and 231+nMPG cell survival was calculated based on the plating efficiency of untreated 231+pcDNA cells. The 231+mito-MPG and 231+nMPG cells were more sensitive to MMS at all doses (Fig. 5). Using the one-way ANOVA test, the P s were <0.05 at 0.05, 0.1, and 0.2 mM MMS comparing the transfected cells to the vector control cells. There was

a statistically significant difference ($P < 0.05$) in the plating efficiency without drug treatment between 231+pcDNA and the 231+mito-MPG cells using the one-way ANOVA test. There were also significant differences ($P < 0.05$) upon comparing the 231+mito-MPG cells and 231+nMPG cells at 0 dose, 0.05, 0.1, and 0.2 mM MMS. Although the MPG activity of the 231+mito-MPG cells was \sim 2-fold less than the 231+nMPG cells (Table 1), the cell sensitivity was even greater.

Comparison of the Slopes of the Cell Survival Curves. To better compare and analyze the effect of overexpressing mito-MPG and nMPG on the MDA-MB231 cells, the data points from the cell survival curves were used to calculate linear regression for the data shown in Fig. 5C. The comparisons of the three slopes generated from these lines were significantly different ($P < 0.0001$) using the χ^2 test with two degrees of freedom. The slopes of 231+pcDNA cells versus 231+mito-MPG cells and 231+mito-MPG cells versus 231+nMPG were significantly different ($P < 0.0001$) using a standard t test. However, the slopes of 231+pcDNA cells versus 231+nMPG cells were not significantly different ($P = 0.254$) using the standard t test. The significantly different slopes of the 231+mito-MPG cells and the 231+nMPG cells implied that the mechanism(s), which the cells were being sensitized to MMS, was also different.

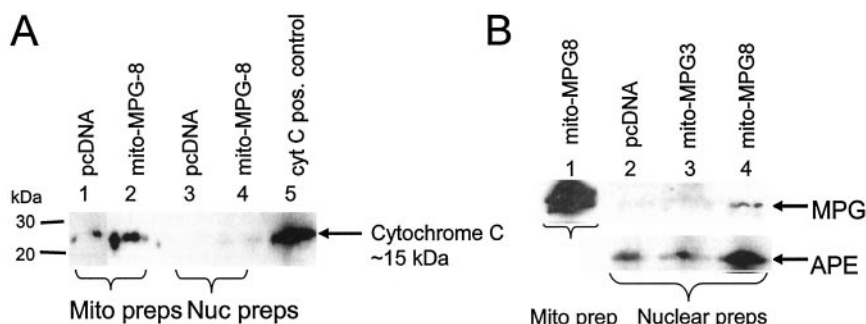
KF of 231+mito-MPG and 231+nMPG Cells. Using the percentage of cells that were killed divided by the units of activity, we defined an arbitrary value, the KF to determine the relevant effect of the nuclear versus mitochondrial-targeted MPG. Assuming that the MPG activity does not change after treatment with MMS, the KF was calculated for all of the doses tested (0.05, 0.1, and 0.2 mM; Table 2). The KF values clearly demonstrated that even with greater than 2-fold higher MPG activity in the 231+nMPG cells (KF = 1.01), the 231+mito-MPG cells are more sensitive without drug treatment (KF = 5.89). However, the KF of the 231+nMPG cells after treatment with 0.2 mM MMS was 4.06, compared with the 231+mito-MPG cells KF of 10.19. The 231+nMPG cells' KF was 4-fold higher after drug treatment compared with the 231+nMPG cells without drug treatment. The 231+mito-MPG cells' KF was 1.73-fold higher after drug treatment compared with the 231+mito-MPG cells without drug treatment. Increasing the amount of MPG in the nucleus did decrease the cells' survival without drug treatment, but a greater

Table 1 Relative activities of the MDA-MB231 cells transfected with pcDNA-mito-MPG or pcDNA-nMPG

Activity units are pmol of substrate/mg of protein normalized to the MDA-MB231 vector control cells.

Cell line	MPG Activity
MDA-MB231	1.0
mito-MPG no. 2	10.4
mito-MPG no. 3	6.1
mito-MPG no. 8	9.6
MPG no. 2	23.0
MPG no. 12	20.0

Fig. 4. Mitochondrial MPG is targeted to the mitochondria in the 231+mito-MPG cells. **A**, Western blot analysis of cytochrome *c* protein (20 μ g) from the mitochondria (Lanes 1 and 2) and nuclei (Lanes 3 and 4) from 231+mito-MPG cell line 8. **B**, Western blot analysis of protein (10 μ g) from the mitochondria (Lane 1) and nuclei (Lanes 2-4) of the 231+mito-MPG cell line 8. The top panel was probed with polyclonal MPG antibody, and the bottom panel was probed with monoclonal Ape1/ref-1 antibody to demonstrate that the lanes did contain nuclear protein.



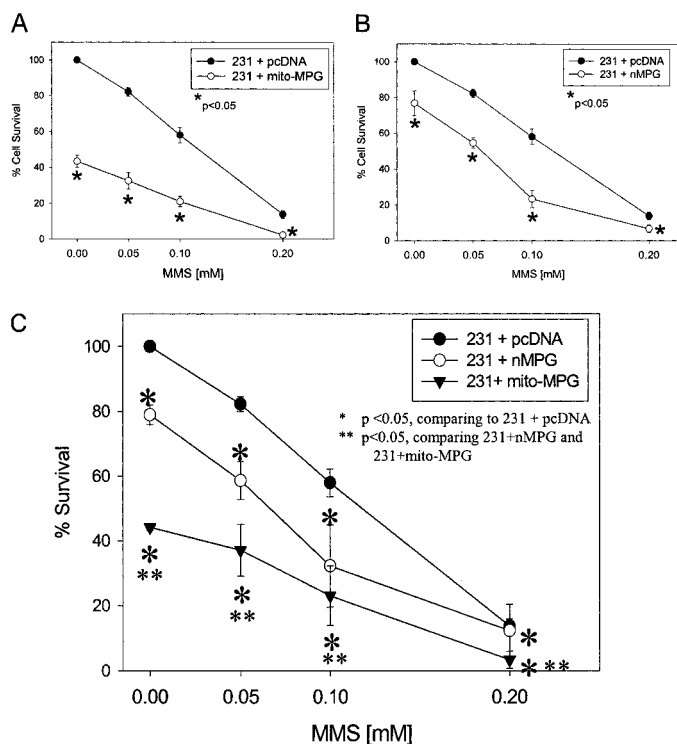


Fig. 5. Targeting MPG to the mitochondria additionally sensitizes the cells to MMS. **A**, effect of mito-MPG overexpression on the cytotoxicity of MMS. The survival percentages are shown as the mean \pm SE of at least 6 separate experiments. **B**, effect of nMPG overexpression on the cytotoxicity of MMS. The survival percentages are shown as the mean \pm SE of at least six separate experiments. **C**, combining the cell survival curves for the percentage of survival of the 231+mito-MPG cells and the 231+nMPG cells after exposure to the same doses of MMS.

induction of sensitivity was seen with drug treatment. Increasing the amount of MPG in the mitochondria dramatically affected the cells' overall survival without drug treatment. In response to the alkylating agent MMS, increasing the amount of MPG in the mitochondria did not induce the sensitivity as seen in the 231+nMPG cells, presumably because so many of the cells were already undergoing cell death even without drug treatment (Fig. 6). These differences are presumably because of a "gene effect," *i.e.*, nuclear *versus* mitochondrial targeting of MPG as opposed to a drug (MMS) effect.

Apoptosis Studies with Annexin-V-FITC Staining. Because of the increase in sensitivity to MMS and other agents, the question of how the cells were dying was analyzed. To investigate this, the cells were treated with MMS, stained with PI and Annexin-V-FITC, and analyzed by flow cytometry. As shown in Fig. 6A, flow cytometry data demonstrated a shift in Annexin-positive cells in 231+mito-MPG and 231+nMPG after treatment with MMS. These results

demonstrated that there was an increase in the percentage of apoptotic cells in 231+mito-MPG and 231+nMPG cells, and the data are represented graphically in Fig. 6B. Consistent with the cell survival data shown previously (Fig. 5), there was also a statistically significant difference ($P < 0.05$) in the percentage of apoptotic cells when comparing the untreated 231+pcDNA and the 231+mito-MPG cells (Fig. 6B). At the 0.1 mM dose of MMS, the percentage of apoptotic cells in 231+mito-MPG and 231+nMPG cells was statistically significant ($P < 0.05$) when compared with 231+pcDNA cells. It appeared that 231+mito-MPG cells have a larger percentage of cells undergoing apoptosis at this dose than 231+nMPG cells, but the difference was not statistically significant. At the 0.2 mM dose of MMS, again both 231+mito-MPG and 231+nMPG cells were statistically significant ($P < 0.05$) when compared with the 231+pcDNA cells using the one-way ANOVA test.

Apoptosis and Cell Morphology Using a Confocal Microscope. The 231+pcDNA, 231+mito-MPG, and 231+nMPG cells were also visualized using confocal microscopy, and an increase in the percentage of cells undergoing apoptosis was evident after MMS treatment for 48 continuous h in 231+mito-MPG and in 231+nMPG cells (Fig. 6A). Interestingly, the confocal analysis also confirmed the cell survival assays and the Annexin-V-FITC staining that demonstrated an increase in apoptosis in 231+mito-MPG cells without drug treatment (Fig. 6).

Caspase-3 Activity Assays. To further explore the mechanism of cell death occurring in 231+nMPG and 231+mito-MPG cells, a second assay for apoptosis was used. As an indication of apoptosis, the activation of the caspase cascade was measured through the caspase-3 enzyme activity in cell lysates. Consistent with the colony forming data and the Annexin-V-FITC staining, the caspase assay demonstrated an increase in caspase-3 activity in the drug-treated 231+mito-MPG and 231+nMPG cells (data not shown). However, the 231+mito-MPG cells did not show an increase in caspase-3 activity at the zero dose in this assay.

DISCUSSION

In previous overexpression experiments with nuclear MPG, cells with increased MPG expression were sensitized to alkylating agents (33, 34, 45, 46). We have confirmed the finding and also partially analyzed how the cells were dying. These results suggest that overexpression of MPG results in more apurinic sites and/or gapped DNA, which would lead to a higher incidence of sister chromatid exchange, replication blocks, and double-strand breaks leading to an apoptosis-induced death (34, 46). To begin to additionally understand how MPG functions in the BER pathway in the mitochondria and to investigate if we could enhance the killing of tumor cells, we added a mitochondrial-targeting sequence to MPG and overexpressed this protein in the mitochondria. As demonstrated in Figs. 5 and 6, the 231+mito-MPG

Table 2 Comparison of KF of mito-MPG- and nMPG-overexpressing cells

MPG activity is in units of pmol substrate/mg protein normalized back to MDA-MB231 vector control cells. The KF is defined as the percentage of kill of the MPG- or mito-MPG-overexpressed cells divided by the relative MPG activity of the MPG- or mito-MPG-overexpressing cells.

Cells	% kill \pm SE	Relative MPG activity ^a	KF	Fold increase of the KF from 0 to X dose MMS
mito-MPG8—0 mM MMS	56.9 \pm 3.3	9.6	5.9	N/A
mito-MPG8—0.05 mM MMS	67.5 \pm 4.6	9.6	7.0	1.4
mito-MPG8—0.1 mM MMS	79.0 \pm 2.8	9.6	8.2	1.2
mito-MPG8—0.2 mM MMS	97.8 \pm 0.4	9.6	10.2	1.7
MPG2—0 mM MMS	23.2 \pm 6.9	23	1.0	N/A
MPG2—0.5 mM MMS	45.5 \pm 2.8	23	2.0	2.0
MPG2—0.1 mM MMS	76.7 \pm 4.9	23	3.3	3.3
MPG2—0.2 mM MMS	93.4 \pm 2.2	23	4.1	4.0

^a Assuming MPG activity does not change after treatment with MMS.

^b N/A, not applicable.

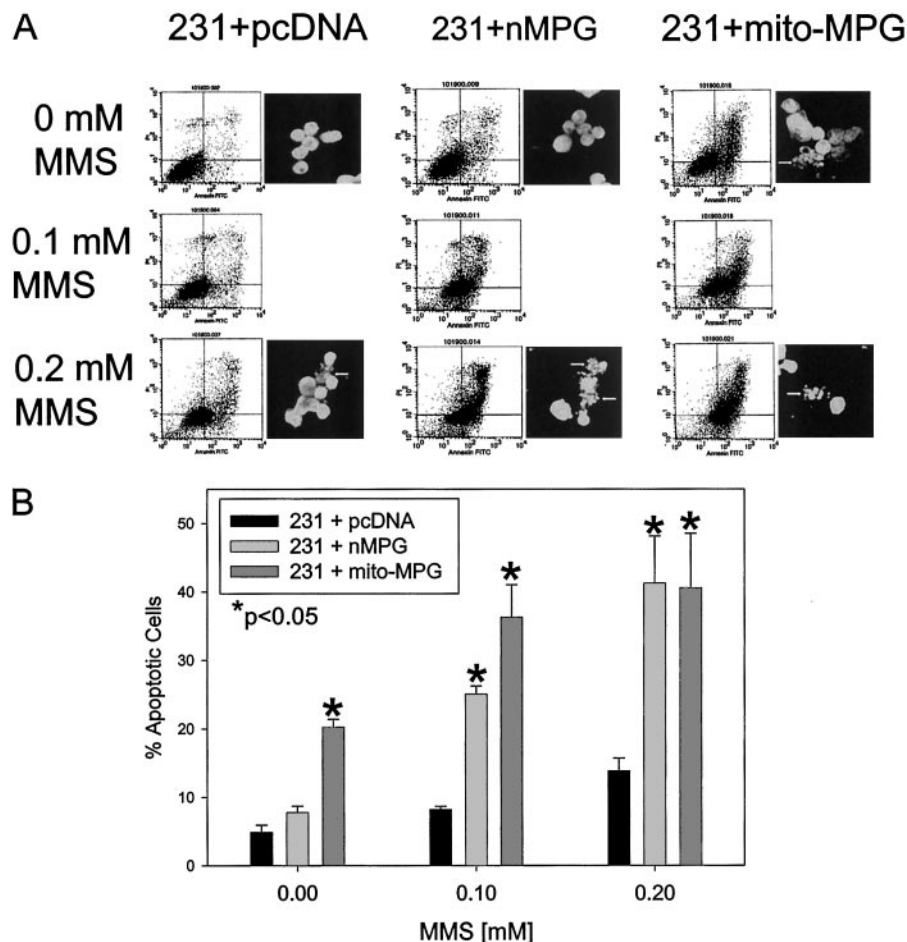


Fig. 6. The number of cells undergoing apoptosis in the mito-MPG-overexpressing cells and the nMPG-overexpressing cells after MMS treatment was significantly higher than the number of vector control cells undergoing apoptosis. *A*, dot plots of 231 + pcDNA, 231 + mito-MPG, and 231 + nMPG cells after treatment with MMS. The x axis is Annexin-V-FITC, and the y axis is PI for all graphs represented. Cells undergoing apoptosis are Annexin-V+, PI- in the lower right quadrant. Additionally, confocal microscopy analysis of 231 cells, 231 + nMPG, and 231 + mito-MPG demonstrating increased apoptosis in the overexpressing MPG cell lines. Arrows are pointing to apoptotic bodies. *B*, graphical representation of the percentage of cells undergoing apoptosis in 231 + mito-MPG and 231 + nMPG cells after treatment with MMS. The average of three independent experiments is represented.

cells were dramatically sensitized when treated with MMS. Statistically significant differences were found between 231 + mito-MPG cells and 231 + nMPG cells at all doses tested (Fig. 5). Another interesting result involved the observation that there was significant cell death without drug treatment. The linear regression data from this cell survival curve demonstrated that the slope of the 231 + mito-MPG cells is statistically different ($P < 0.0001$) from the 231 + pcDNA cells and the 231 + nMPG cells; however, the slope of the 231 + nMPG cells and the 231 + pcDNA cells are not statistically different. Additionally, this difference in slope is because of the fact that the mitochondrially targeted cells were already under duress given that 60% were dying, even without drug treatment. This was evidenced by the Annexin-V staining and cell morphology studies showing increased apoptosis of the cells expressing the mito-MPG as compared with the vector or nMPG-targeted cells. This may also indicate that 231 + mito-MPG cells are activating different or additional pathways of apoptosis than 231 + nMPG cells. If the overexpression of mito-MPG is imbalancing the BER pathway in mitochondria, this imbalance may be more detrimental to the cells than the damage from MMS. This could help to explain why 231 + mito-MPG cells are so much more sensitive when untreated.

We and others hypothesize that overexpression of MPG causes an imbalance in the BER pathway (34). The imbalance can result in cell death through an accumulation of AP sites or single-strand and double-strand breaks. If the ratio of base removal (MPG activity) is higher than the incision activity of Ape1/ref-1, AP sites accumulate and can persist. Furthermore, if the ratio of incision is higher than the dRPase activity of β -pol, the polymerization by β -pol, or sealing the nicks by ligase, the DNA remains nicked and gapped (47). AP site

accumulation could be involved in the mechanism of cellular sensitivity seen with MPG overexpression and treatment with alkylating agents. High levels of the MPG protein in either the mitochondria or the nucleus could result in an accumulation of AP sites after MMS treatment by increasing the rate of removal of the alkylated bases. In addition to increasing the number of AP sites after treatment with DNA damaging agents, MPG has also been shown to remove intact, undamaged bases at a biologically significant rate (48). At higher than physiological levels of MPG, this promiscuity could become significant, removing both intact and damaged bases. MPG also removes the etheno adduct of purines that results endogenously from lipid peroxidation (49). With increased MPG, there would be an increase in the removal of this adduct and an increase in AP sites. With the increase in AP sites, the probability of mutagenesis, blocking DNA replication, and/or stimulating topoisomerase II also increases (50–52).

AP site accumulation may be one of the mechanisms affecting the viability of the mito-MPG-overexpressing cells. Because of the difference in slope and cellular sensitivity when compared with the nMPG-overexpressing cells, it appears there are additional mechanisms contributing to the mito-MPG-overexpressing cells' sensitivity to MMS. In Fig. 6A, the slope of the line from 231 + mito-MPG cells does not appear to be as steep as the line from 231 + nMPG cells, although 231 + mito-MPG cells are sensitized more without drug treatment. This is confirmed by the KF of 231 + mito-MPG and 231 + nMPG cells (Table 2). Although difficult to explain, one possibility is that in the population of cells that exist, those cells that have high levels of mito-MPG have already begun the cascade toward programmed cell death before drug treatment. After drug treatment, the resulting cells are actually a more resistant population because of

the highest expressing cells already initiating apoptosis. This hypothesis is supported by the fact that in 231 + mito-MPG cells that have not been treated with MMS, there is an increase in the number of cells undergoing apoptosis as detected by staining with Annexin-V and analysis with a confocal microscope (Fig. 6) but not showing an increase in caspase-3 activity (data not shown). This lack of caspase-3 activation suggests an alternate mechanism of inducing apoptosis perhaps through caspase-6 or caspase-7. Because MPG can remove undamaged bases at a biologically significant rate (48), more than likely the high levels of MPG protein in the mitochondria leads to a promiscuity allowing the removal of undamaged purines, resulting in many AP sites without drug treatment. Although accumulation of AP sites has been discussed as a probable mechanism for the sensitization observed with nuclear MPG overexpression, this could have an even greater or different effect in mitochondria for several reasons. Because mtDNA does not have long sequences of bases that are noncoding, it contains no introns and is not protected by histones (12), there is a greater chance that the genes encoding proteins involved in the electron transport chain will accumulate mutations. The proteins involved in the respiratory chain complex would either not be synthesized or mutant forms would be synthesized. It is believed if the electron transport chain were not functioning properly, more ROS would be generated, leading to more DNA damage and a decrease in the cells' energy level. It should also be remembered that MPG recognizes ϵ A adducts in DNA (49). These adducts are a consequence of lipid oxidation that could be elevated in the mitochondria after elevated DNA damage. In fact, this supports a vicious cycle effect of increased mtDNA damage leading to increased electron transport chain defects and an increase in ROS leading to more DNA damage. Although we have no direct evidence for this at present, the much higher level of spontaneous cell killing in the mitochondrial-targeted cells compared with the nuclear targeted cells may be an indicator of this scenario. Alternatively, more oxidative damage and a lower energy supply could open the mitochondrial permeability transition pore and lead to apoptosis (53, 54). Proteins in the inner membrane of the mitochondria such as cytochrome *c* and apoptosis-inducing factor are released upon translocation of proteins to the mitochondria membrane and opening of the mitochondrial permeability transition pore, and the cascade of apoptotic events begins (53, 55, 56). An increase in apoptosis has been observed in 231 + mito-MPG cells at all drug doses (Fig. 6). Perhaps the increase in AP sites in mtDNA causes enough mutations or blocks to the replication polymerase to compromise the mitochondria's ability to generate ATP eventually resulting in apoptosis.

To explain the dramatic increase in cellular sensitivity and percentage of cells undergoing apoptosis in the mito-MPG- and nMPG-transfected lines, we hypothesized that overexpression of MPG caused more bases, undamaged and damaged, to be removed. The resulting AP sites accumulated and persisted causing 231 + mito-MPG and 231 + nMPG cells to be sensitized with and without drug treatment. This sensitization has applications in tumor-targeted gene therapy protocols to induce tumor cell killing. The recent finding that MPG interacts with nucleotide excision repair proteins, hHR23A and B, also has implications in combination therapy approaches (57). For example, overexpression of mito-MPG and/or MPG could result in increased kill of tumor cells using lower doses of harmful alkylating agents such as temozolomide and cross-linking agents such as cisplatin. Furthermore, the use of lower doses of chemotherapeutic agents, which would decrease the emergence of drug-resistant tumor cells and decrease the need for stem-cell support, leading to an increased patient response and a better quality of life for the patient.

ACKNOWLEDGMENTS

We thank Dr. Mike Southall and Qiaofang Yi from Dr. Jeff Travers Lab (Department of Dermatology, Indiana University School of Medicine) for technical help with the caspase-3 activity assay. We also thank Allison Dobson (University of South Alabama, Birmingham, AL) for the mitochondrial isolation procedure, Dr. Tim O'Connor for MPG antibody, and Dr. Sin-Ho Jung (IU Cancer Center) for help on statistical analyses.

REFERENCES

- Barzilay, G., and Hickson, I. D. Structure and function of apurinic/apyrimidinic endonucleases. *Bioessays*, *17*: 713–719, 1995.
- Barzilay, G., Mol, C. D., Robson, C. N., Walker, L. J., Cunningham, R. P., Tainer, J. A., and Hickson, I. D. Identification of critical active-site residues in the multifunctional human DNA repair enzyme HAP1. *Nat. Struct. Biol.*, *2*: 561–568, 1995.
- Mol, C., Izumi, T., Mitra, S., and Tainer, J. A. Structure and function of the multifunctional DAN-repair enzyme exonuclease III. *Nature (Lond.)*, *374*: 381–386, 1995.
- Demple, B., and Harrison, L. Repair of oxidative damage to DNA: enzymology and biology. *Annu. Rev. Biochem.*, *63*: 915–948, 1994.
- Doetsch, P., and Cunningham, R. The enzymology of apurinic/apyrimidinic endonucleases. *Mutat. Res.*, *236*: 173–201, 1990.
- Mitra, S. T. H., Roy, R., Ikeda, S., Biswas, T., Lock, J., Boldogh, I., and Izumi, T. Complexities of DNA base excision repair in mammalian cells. *Mol. Cells*, *7*: 305–312, 1997.
- Matsumoto, Y., and Kim, K. Excision of deoxyribose phosphate residues by DNA polymerase β during DNA repair. *Science (Wash. DC)*, *269*: 699–702, 1995.
- Piersen, C. E., Prasad, R., Wilson, S. H., and Lloyd, R. S. Evidence for an amino intermediate in the DNA polymerase β deoxyribose phosphate excision reaction. *J. Biol. Chem.*, *271*: 17811–17815, 1996.
- Singhal, R. K., Prasad, R., and Wilson, S. H. DNA polymerase β conducts the gap-filling step in uracil-initiated base excision repair in a bovine testis nuclear extract. *J. Biol. Chem.*, *270*: 949–957, 1995.
- Srivastava, D., Berg, B. J., Prasad, R., Molina, J. T., Beard, W. A., Tomkinson, A. E., and Wilson, S. H. Mammalian abasic site base excision repair Identification of the reaction sequence and rate-determining steps. *J. Biol. Chem.*, *273*: 21203–21209, 1998.
- Anderson, S., Bankier, A. T., Barrell, B. G., de Bruijn, M. H., Coulson, A. R., Drouin, J., Eperon, I. C., Nierlich, D. P., Roe, B. A., Sanger, F., Schreier, P. H., Smith, A. J., Staden, R., and Young, I. G. Sequence and organization of the human mitochondrial genome. *Nature (Lond.)*, *290*: 457–465, 1981.
- LeDoux, S. P., Wesley, J. P., Driggers, B., Hollensworth, S., and Wilson, G. L. Repair of alkylation and oxidative damage in mitochondrial DNA. *Mutat. Res.*, *434*: 149–159, 1999.
- Wallace, D. C. Mitochondrial genetics: a paradigm for aging and degenerative diseases? *Science (Wash. DC)*, *256*: 628–632, 1992.
- Frenkel, K. Carcinogen-mediated oxidant formation and oxidative DNA damage. *Pharmac. Ther.*, *53*: 127–166, 1992.
- Richter, C. Do mitochondrial DNA fragments promote cancer and aging? *FEBS Lett.*, *241*: 1–5, 1988.
- Gerbitz, K. D. Does the mitochondrial DNA play a role in the pathogenesis of diabetes? *Diabetologia*, *35*: 1181–1186, 1992.
- Yakes, F. M. a. B. V. H. Mitochondrial DNA damage is more extensive and persists longer than nuclear DNA damage in human cells following oxidative stress. *Proc. Natl. Acad. Sci. USA*, *94*: 514–519, 1997.
- LeDoux, S. P., Wilson, G. L., Beecham, E. J., Stevnsner, T., Wassermann, K., and Bohr, V. A. Repair of mitochondrial DNA after various types of DNA damage in Chinese hamster ovary cells. *Carcinogenesis (Lond.)*, *13*: 1967–1973, 1992.
- Zastawny, T. H., Dabrowska, M., Jaskolski, T., Klimarczyk, M., Kulinski, L., Koszela, A., Szczesniwicz, M., Sliwinska, M., Witkowski, P., and Olinski, R. Comparison of oxidative base damage in mitochondrial and nuclear DNA. *Free Radic. Biol. Med.*, *24*: 722–725, 1998.
- Myers, K. A., Saffhill, R., and O'Conner, P. J. Repair of alkylated purines in the hepatic DNA of mitochondria and nuclei in the rat. *Carcinogenesis (Lond.)*, *9*: 285–292, 1988.
- Wunderlich, V., Schutt, M., Bottger, M., and Graffi, A. Preferential alkylation of mitochondrial deoxyribonucleic acid by *N*-methyl-*N*-nitrosourea. *Biochem. J.*, *118*: 99–109, 1970.
- Brown, W. M., George, M., Jr., and Wilson, A. C. Rapid evolution of animal mitochondrial DNA. *Proc. Natl. Acad. Sci. USA*, *76*: 1967–1971, 1979.
- Wallace, D. C. Mitochondrial DNA mutations and neuromuscular disease. *Trends Genet.*, *5*: 9–13, 1989.
- Driggers, W., LeDoux, S., and Wilson, G. Repair of oxidative damage within the mitochondrial DNA of R1Nr 38 cells. *J. Biol. Chem.*, *268*: 22042–22045, 1993.
- Takao, M., Aburatani, H., Kobayashi, K., and Yasui, A. Mitochondrial targeting of human DNA glycosylases for repair of oxidative DNA damage. *Nucleic Acids Res.*, *26*: 2917–2922, 1998.
- Nilsen, H., Otterlei, M., Haug, T., Solum, K., Nagelhus, T. A., Skorpen, F., and Krokan, H. E. Nuclear and mitochondrial uracil-DNA glycosylases are generated by alternative splicing and transcription from different positions in the UNG gene. *Nucleic Acids Res.*, *25*: 750–755, 1997.

27. Tomkinson, A. E., Bonk, R. T., and Linn, S. Mitochondrial endonuclease activities specific for apurinic/apyrimidinic sites in DNA from mouse cells. *J. Biol. Chem.*, 263: 12532–12537, 1988.
28. Pinz, K. G., and Bogenhagen, D. F. Efficient repair of abasic sites in DNA by mitochondrial enzymes. *Mol. Cell. Biol.*, 18: 1257–1265, 1998.
29. Longley, M. J., Prasad, R., Srivastava, D. K., Wilson, S. H., and Copeland, W. C. Identification of 5'-deoxyribose phosphate lyase activity in human DNA polymerase γ and its role in mitochondrial base excision repair *in vitro*. *Proc. Natl. Acad. Sci. USA*, 95: 12244–12248, 1998.
30. Pirsell, M., and Bohr, V. A. Methyl methanesulfonate adduct formation and repair in the DHFR gene and in mitochondrial DNA in hamster cells. *Carcinogenesis (Lond.)*, 14: 2105–2108, 1993.
31. Pettepher, C. C., LeDoux, S. P., Bohr, V. A., and Wilson, G. L. Repair of alkali-labile sites within the mitochondrial DNA of R1N3 cells after exposure to the nitrosourea streptozotocin. *J. Biol. Chem.*, 266: 3113–3117, 1991.
32. Frosina, G. Overexpression of enzymes that repair endogenous damage to DNA. *Eur. J. Biochem.*, 267: 2135–2149, 2000.
33. Ibeanu, G., Hartenstein, B., Dunn, W. C., Chang, L. Y., Hofmann, E., Coquerelle, T., Mitra, S., and Kaina, B. Overexpression of human DNA repair protein *N*-methylpurine-DNA glycosylase results in the increased removal of *N*-methylpurines in DNA without a concomitant increase in resistance to alkylating agents in Chinese hamster ovary cells. *Carcinogenesis (Lond.)*, 13: 1989–1995, 1992.
34. Coquerelle, T., Dosch, J., and Kaina, B. Overexpression of *N*-methylpurine-DNA glycosylase in Chinese hamster ovary cells renders them more sensitive to the production of chromosomal aberrations by methylating agents: a case of imbalanced DNA repair. *Mutat. Res.*, 336: 9–17, 1995.
35. Shimoda-Matsubayashi, S., Matsumine, H., Kobayashi, T., Nakagawa-Hattori, Y., Shimizu, Y., and Mizuno, Y. Structural dimorphism in the mitochondrial targeting sequence in the human manganese superoxide dismutase gene. A predictive evidence for conformational change to influence mitochondrial transport and a study of allelic association in Parkinson's disease. *Biochem. Biophys. Res. Commun.* 226: 561–565, 1996.
36. Dobson, A. W., Xu, Y., Kelley, M. R., LeDoux, S. P., and Wilson, G. L. Enhanced mitochondrial DNA repair and cellular survival after oxidative stress by targeting the human 8-oxoguanine glycosylase repair enzyme to mitochondria. *J. Biol. Chem.*, 275: 37518–37523, 2000.
37. Kelley, M. R., Cheng, L., Foster, R., Tritt, R., Jiang, J., Broshears, J., and Koch, M. Elevated and altered expression of the multifunctional DNA base excision repair and redox enzyme Ape1/ref-1 in prostate cancer. *Clin. Cancer Res.*, 7: 824–830, 2001.
38. Robertson, K. A., Bullock, H. A., Xu, Y., Tritt, R., Zimmerman, E., Ulbright, T. M., Foster, R. S., Einhorn, L. H., and Kelley, M. R. Altered expression of Ape1/ref-1 in germ cell tumors and overexpression in NT2 cells confers resistance to bleomycin and radiation. *Cancer Res.*, 61: 2220–2225, 2001.
39. Chen, D. S., Herman, T., and Demple, B. Two distinct human DNA diesterases that hydrolyze 3'-blocking deoxyribose fragments from oxidized DNA. *Nucleic Acids Res.*, 19: 5907–5914, 1991.
40. Sambrook, J. E. F., and Maniatis, T. *Molecular Cloning: A Laboratory Manual*. Cold Spring Harbor, NY, 1989.
41. Roy, R., Biswas, T., Hazra, T. K., Roy, G., Grabowski, D. T., Izumi, T., Srinivasan, G., and Mitra, S. Specific interaction of wild-type and truncated mouse *N*-methylpurine-DNA glycosylase with ethenoadenine-containing DNA. *Biochemistry*, 37: 580–589, 1998.
42. Vermes, I., Haanen, C., Steffens-Nakken, H., and Reutelingsperger, C. A novel assay for apoptosis. Flow cytometric detection of phosphatidylserine expression on early apoptotic cells using fluorescein labelled Annexin V. *J. Immunol. Methods*, 184: 39–51, 1995.
43. Nicholson, D. W., Ali, A., Thornberry, N. A., Vaillancourt, J. P., Ding, C. K., Gallant, M., Gareau, Y., Griffin, P. R., Labelle, M., Lazebnik, Y. A., Munday, N. A., Raju, S. M., Smulson, M. E., Yamin, T., Yu, V. L., and Miller, D. K. Identification and inhibition of the ICE/CED-3 protease necessary for mammalian apoptosis. *Nature (Lond.)*, 376: 37–43, 1995.
44. Anne, J. M., Martin, S. J., Bissonnette, R. P., Mahboubi, A., Shi, Y., Mogil, R. J., Nishioka, W. K., and Green, D. R. *Methods in Cell Biology*, Vol. 46, pp. 153–185. New York: Academic Press, 1995.
45. Grombacher, T., Tomicic, M., Digweed, M., and Kaina, B. Overexpression of cDNA encoding FANCC, SPHAR, MPG, SNM1 or HA 3611 does not render CHO cells more resistant to DNA crosslinking agents. *Anticancer Res.*, 19: 1729–1735, 1999.
46. Calleja, F., Jansen, J. G., Vrieling, H., Laval, F., and van Zeeland, A. A. Modulation of the toxic and mutagenic effects induced by methyl methanesulfonate in Chinese hamster ovary cells by overexpression of rat *N*-alkylpurine-DNA glycosylase. *Mutat. Res.*, 425: 185–194, 1999.
47. Wyatt, M. D., Allan, J. M., Lau, A. Y., Ellenberger, T. E., and Samson, L. D. 3-Methyladenine DNA glycosylases: structure, function, and biological importance. *Bioessays*, 21: 668–676, 1999.
48. Berdal, K. G., Johansen, R. F., and Seeberg, E. Release of normal bases from intact DNA by a native DNA repair enzyme. *EMBO J.*, 17: 363–367, 1998.
49. Dosaanjh, M. K., Roy, R., Mitra, S., and Singer, B. 1. N6-ethenoadenine is preferred over 3-methyladenine as substrate by a cloned human *N*-methylpurine-DNA glycosylase (3-methyladenine-DNA glycosylase). *Biochemistry*, 33: 1624–1628, 1994.
50. Loeb, L. A., and Preston, B. D. Mutagenesis by apurinic/apyrimidinic sites. *Ann. Rev. Genet.*, 20: 201–230, 1986.
51. Schaaper, R., Kunkel, T. A., and Loeb, L. A. Infidelity of DNA synthesis associated with bypass of apurinic sites. *Proc. Natl. Acad. Sci. USA*, 80: 487–491, 1983.
52. Kingma, P. S., and Osheroff, N. Apurinic sites are position-specific topoisomerase II poisons. *J. Biol. Chem.*, 272: 1148–1155, 1997.
53. Wallace, D. C. Mitochondrial diseases in man and mouse. *Science (Wash. DC)*, 283: 1482–1488, 1999.
54. Druzhyina, N., Smulson, M. E., Ledoux, S. P., and Wilson, G. L. Poly(ADP-ribose) polymerase facilitates the repair of *N*-methylpurines in mitochondrial DNA. *Diabetes*, 49: 1849–1855, 2000.
55. Brenner, C., and Kroemer, G. Apoptosis. Mitochondria: the death signal integrators [comment]. *Science (Wash. DC)*, 289: 1150–1151, 2000.
56. Green, D. R., and Reed, J. C. Mitochondria and apoptosis. *Science (Wash. DC)*, 281: 1309–1312, 1998.
57. Miao, F., Bouziane, M., Dammann, R., Masutani, C., Hanaoka, F., Pfeifer, G. P., and O'Connor, T. R. 3-Methyladenine-DNA glycosylase (MPG protein) interacts with human RAD23 proteins. *J. Biol. Chem.*, 275: 28433–28438, 2000.